Monitoring of band gap and magnetic state of graphene nanoribbons through vacancies

M. Topsakal,[1] E. Aktürk,[1] H. Sevinçli,[1,2] and S. Ciraci[1,2,*]

[1] *UNAM-Institute of Materials Science and Nanotechnology, Bilkent University, Ankara 06800, Turkey*
[2] *Department of Physics, Bilkent University, Ankara 06800, Turkey*

Using first-principles plane wave calculations we predict that electronic and magnetic properties of graphene nanoribbons can be affected by defect-induced itinerant states. The band gaps of armchair nanoribbons can be modified by hydrogen saturated holes. Defects due to periodically repeating vacancy or divacancies induce metallization, as well as magnetization in non-magnetic semiconducting nanoribbons due to the spin-polarization of local defect states. Antiferromagnetic ground state of semiconducting zigzag ribbons can change to ferrimagnetic state upon creation of vacancy defects, which reconstruct and interact with edge states. Even more remarkable is that all these effects of vacancy defects are found to depend on their geometry and position relative to edges. It is shown that these effects can, in fact, be realized without really creating defects

PACS numbers: 73.22.-f, 75.75.+a, 75.70.Ak

I. INTRODUCTION

Its unusual electronic energy band structure and charge carriers resembling massless Dirac Fermions have made graphene honeycomb structure an active field of research[1,2,3,4,5]. Quasi 1D graphene ribbons have even more interesting electronic and magnetic properties depending on their size and symmetry[6]. These are edge states of zigzag ribbons with opposite spin polarization[7] and band gaps varying with the width of the ribbon[8].

Theoretical studies have predicted that energetic electrons and ions can induce polymorphic atomic defects , such as vacancies in graphene[9]. Using high-resolution TEM the observation of vacancies have been reported[10]. Recent studies have shown that vacancies created on two-dimensional (2D) graphene by high-energy electron or ion irradiation can induce magnetism in a system consisting of only *sp*-electrons[11,12]. It has been argued that Stoner magnetism with high T_C originates from the spin-polarized extended states induced by the vacancy defects, while RKKY coupling is suppressed. These effects of defects on 1D semiconducting graphene nanoribbons should be more complex and interesting, because their band gap, magnetic state and symmetry are expected to intervene.

Present study based on extensive first-principles as well as empirical tight-binding calculations (ETB) has shown that the band gap and magnetic state of any armchair or zigzag nanoribbons can be modified by single or multiple vacancies (holes). The effects of these defects depend on their symmetry, repeating periodicity and positions. Even if the formation of periodic defects of desired symmetry may not easily be achieved, similar effects can be created through the potential difference across a ribbon applied by periodically arranged tips. When combined with various properties of nanoribbons these results can initiate a number of interesting applications. We believe that our results are important for further studies, since the graphene ribbons can now be produced with precision having widths sub 10 nm[13] and nanodevices can be fabricated thereof[14].

II. MODEL AND METHODOLOGY

We have performed first-principles plane wave calculations within Density Functional Theory (DFT) using PAW potentials[15]. The exchange correlation potential has been approximated by Generalized Gradient Approximation (GGA) using PW91[16] functional both for spin-polarized and spin-unpolarized cases. All structures have been treated within supercell geometry using the periodic boundary conditions. A plane-wave basis set with kinetic energy cutoff of 500 eV has been used. In the self-consistent potential and total energy calculations the Brillouin zone (BZ) is sampled by (1x1x35) special **k**-points for ribbons. This sampling is scaled according to the size of superlattices. All atomic positions and lattice constants are optimized by using the conjugate gradient method where total energy and atomic forces are minimized. The convergence for energy is chosen as 10^{-5} eV between two steps, and the maximum force allowed on each atom is less than 0.02 eV /Å. Numerical plane wave calculations have been performed by using VASP package[17,18]

III. VACANCY DEFECTS IN NANORIBBONS

We start by summarizing the electronic properties of graphene nanoribbons which are relevant for the present study. We will consider hydrogen terminated nanoribbons if it is not stated otherwise. Armchair graphene nanoribbons, AGNR(N) (N being the number of carbon atoms in the primitive unit cell), are non-magnetic semiconductors. The band gap[8,19], E_G, of a bare or hydrogen terminated AGNR(N) is small for $N = 6m-2$ (m being an integer), but from $N = 6m$ to $N = 6m+2$ it increases and passing through a maximum it becomes again small

at the next minimum corresponding to $N = 6m + 4$. As E_G oscillates with N its value shall decrease eventually to zero as $N \to \infty$. Bare and hydrogen terminated zigzag nanoribbons, ZGNR(N), are also semiconductors with E_G decreasing consistently as N increases for $N >$8, but their edge states give rise to antiferromagnetic (AFM) ground state[7]. We will show that these magnetic and electronic properties can be modified by defects originating from vacancies or holes created in those ribbons.

A hole can be created when carbon atoms at the corners of any hexagon of an armchair ribbon are removed and subsequently remaining six two-fold coordinated carbon atoms are terminated with hydrogen atoms. Figure 1 (a) - (b) shows that the electronic structure of AGNR(34) is strongly modified by such a hole which is placed at the center of the ribbon. The hole repeats itself at each supercell which comprises six primitive cells corresponding to a repeat period of l=6. This ribbon having a periodic hole (or defect) is specified as AGNR(N;l) and has non-magnetic ground state. Despite large separation of periodic defect which hinders their direct coupling such a strong modification of the band gap is somehow unexpected. However, it is an indirect effect and occurs since the itinerant (Bloch) states of band edges are modified by the defect. At the end, the direct band gap[19] at the Γ-point has widened from 0.09 eV to 0.40 eV due to a defect situated at the center of the ribbon. AGNR (36) exhibit the same behavior; namely its band gap increases when a similar hole repeats itself at each supercell consisting of six primitive cell. However, in contrast, the band gap of AGNR(38), which is normally larger than that of AGNR(34), is reduced if the same hole is introduced at its center. In addition, states localized around the defect have formed flat bands near the edge of valence and conduction bands because of their reduced coupling.

Moreover, the effect of this defect is strongly dependent on its position relative to the both edges of the nanoribbon as depicted in Fig. 2 (a). As shown in Fig. 2 (b), the changes in band gap depend on N of AGNR (in the family specified as $6m + q$, q being -2, 0 and +2) as well as on the position of the hole. We note that the variation of the band gap with the position of the hole relative to the edges of the ribbon show similar trends for both AGNR (34,6) and AGNR (36;6). However, AGNR (38;6) displays an opposite trend.

ETB calculations indicate that a similar behavior is also obtained in AGNR(N;l)'s having relatively larger N (i.e. N=58, 60, 62) in Fig 2 (c). As expected the effect of the hole on the band gap depends on the repeat periodicity. As shown in Fig 2 (d), the effects of defect decrease with increasing repeat periodicity l. We found that larger holes with different geometry and rotation symmetry can result in diverse electronic structure and confined states. It should be noted that a repeating hole can also modify the mechanical properties. For example, the stiffness of a ribbon is reduced by the presence of a hole. The force constant, $\kappa = \partial^2 E_T/\partial c^2$ (c being the lattice constant) calculated for AGNR(34;6) with a hole

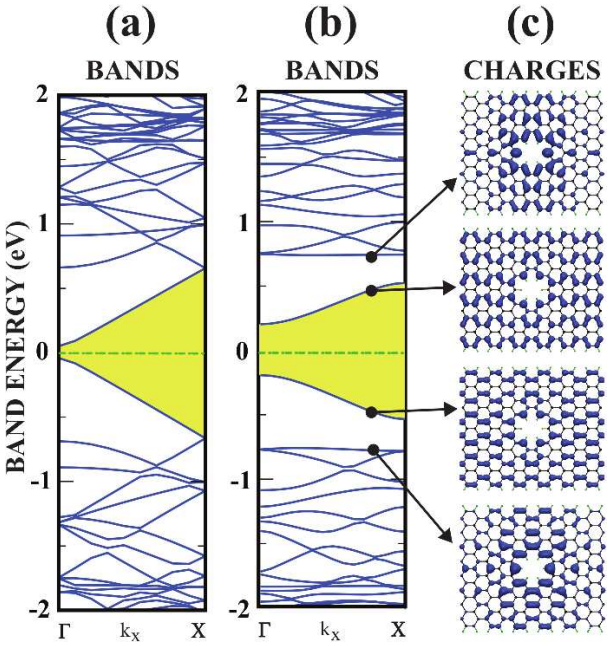

FIG. 1: (Color online)(a) Energy band structures of AGNR(N=34;l=6) with and (b) without a hole consisting of six carbon vacancies. (c) Charge density isosurfaces of selected states. Carbon atoms (represented by black circles), which have coordination number lower than 3 are terminated by hydrogen atoms (represented by small gray circles).

at its center ($\kappa = 6.03$ eV/Å) is found to be smaller than that without a hole κ =7.50 eV/Å).

We now show that different types of vacancies in the same armchair nanoribbon gives rise to different changes in electronic and magnetic properties. A divacancy created in AGNR(22) can cause to a dramatic change in the electronic state of the ribbon when it is repeated with the periodicity of l=5. Such an armchair ribbon is specified as AGNR(22;5). The divacancy first relaxes and forms an eight fold ring of carbon atoms which is adjacent to six hexagons and two pentagons. In Fig. 3 (a) we see that the non-magnetic and semiconducting AGNR(22) with band gap of E_G=0.18 eV becomes a non-magnetic metal, since a flat band derived from the defect occurs below the top of the valance band edge and causes to a metallic state.

The effect of a single carbon vacancy becomes even more interesting. A single vacancy created in AGNR(22) is relaxed and the three-fold rotation symmetry is broken due to Jahn-Teller distortion. At the end, a nine-sided ring forms adjacent to a pentagon as shown in Fig. 3 (b). Owing to the spin-polarization of the sp^2-dangling bond on the two-fold coordinated carbon atom and adjacent orbitals at the defect site the system obtains an unbalanced spin. In fact, the difference of total charge density corresponding to states of different spin states, i.e. $\Delta\rho_T = \rho_T^{\uparrow} - \rho_T^{\downarrow}$ is non-zero and exhibits a distribution shown in Fig. 3 (b). Because of unbalanced spin, AGNR(22;5) gains a net magnetic moment of μ=1 μ_B per

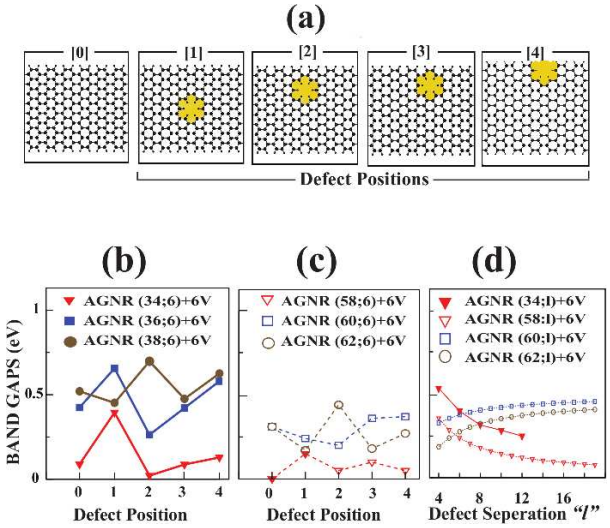

FIG. 2: (Color online) (a) Positions of a hole in the ribbon are indicated by numerals. The nanoribbon without a hole is specified by "0". (b) and (c) Variations of band gaps of AGNR(N,l) with the position of the hole specified as 6V . (d) Variation of band gap with repeat periodicity, l. Results for $N < 58$ are obtained by first-principles calculations.

cell. This attributes a magnetic state to the nanoribbon, which was nonmagnetic otherwise.

Furthermore, the spin degeneracy of some bands related with this defect is broken and spin-up and spin-down bands are split. The dispersive, non-magnetic band at the edge of the valence band becomes partially emptied, since its electrons are transferred to the flat spin bands below. Eventually, the semiconducting ribbon becomes metallic.

Not only armchair, but also zigzag nanoribbons are strongly affected by defects due to single and multiple vacancies. When coupled with the magnetic edge states of the zigzag nanoribbons the vacancy defect brings about additional changes. The magnetic state and energy band structure of these ribbons depend on the type and geometry of the defects. In Fig. 4 (a)-(c), the effect of a defect generated from the single vacancy with a repeat periodicity of l=8 is examined in ZGNR(14;8) for three different positions. The total energy is 0.53 eV lowered when the defect is situated at the edge rather than at the center of the ribbon.

ZGNR(14;8) has a net magnetic moment of μ=1.94 μ_B when the defect is situated at the center of the ribbon and hence its antiferromagnetic ground state has changed to ferrimagnetic state through the magnetic moment of the single vacancy. Otherwise, μ becomes zero, when the position of the defect deviates from the center. For example, in Fig. 4 (b) and (c) the sum of the magnetic moments of the edge states is not zero, but the net magnetic moment per unit cell becomes zero only after the spins of the defect is added. Even if the net magnetic moment μ=0, ZGNR(14,8) does not have an antiferromagnetic ground state due to the presence of single vacancy.

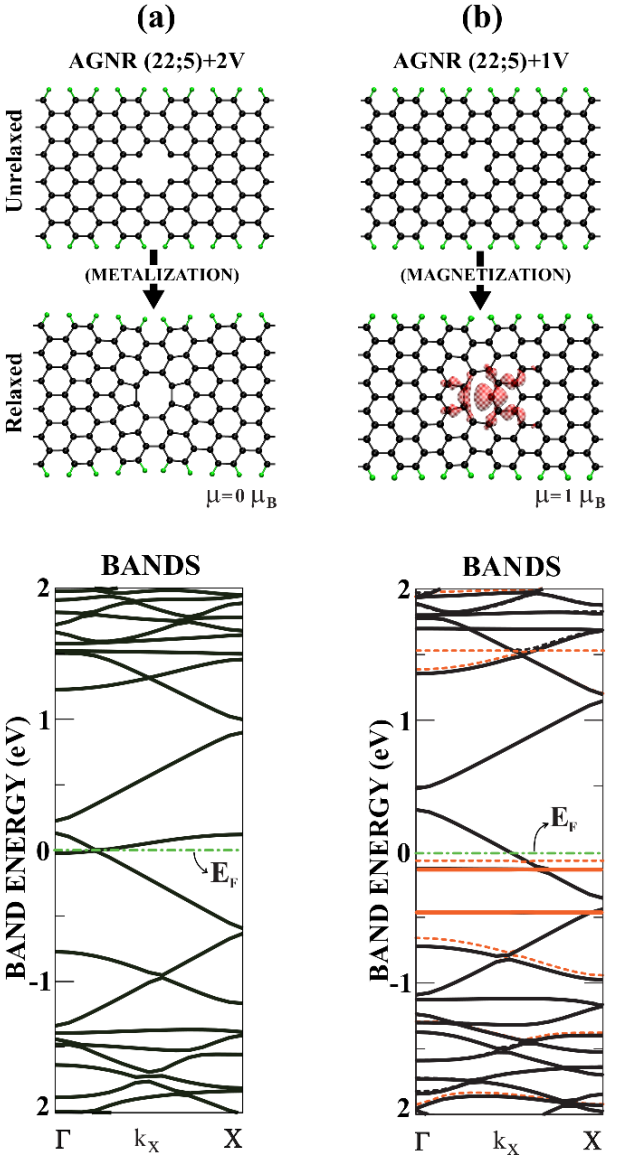

FIG. 3: (Color online)(a) Metallization of the semiconducting AGNR(22) by the formation of divacancies with repeat period of l=5. (b) Magnetization of the non-magnetic AGNR(22) by a defect due to the single carbon atom vacancy with the same repeat periodicity. Isosurfaces around the vacancy corresponding to $\Delta\rho_T$; namely the difference of the total charge density of different spin directions.Solid (blue) and dashed (red) lines are for spin-up and spin-down bands; solid (black) lines are nonmagnetic bands.

The edge states, each normally having equal but opposite magnetic moments, become ferrimagnetic when a defect is introduced. The total magnetic moment of the supercell vanish only after the magnetic moment of defect has been taken into account. Since the spin-degeneracy has been broken, one can define $E_G^{\uparrow}$ and $E_G^{\downarrow}$ for majority and minority spin states. Not only the magnetic state, but also the band gap of zigzag ribbons in Fig. 4 are affected by the symmetry and the position of the defect relative to

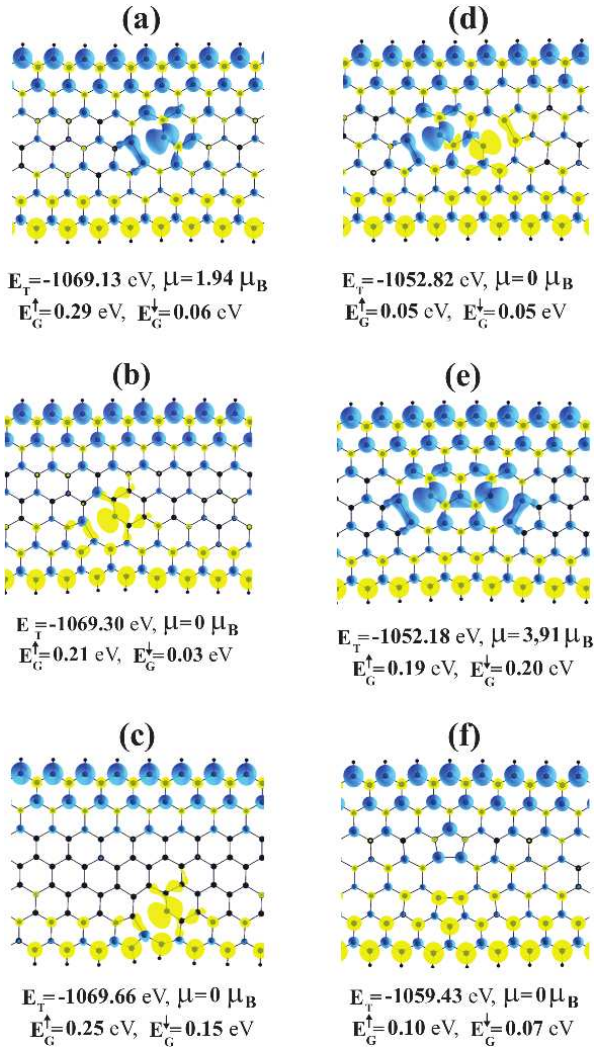

FIG. 4: (Color online) Vacancy and divacancy formation in an antiferromagnetic semiconductor ZGNR(14) with repeat period of l=8. Calculated total energy, E_T (in eV/cell), net magnetic moment, μ (in Bohr magneton μ_B/cell), band gap between spin-up(down) conduction and valence bands, $E_G^{\uparrow(\downarrow)}$) are shown for each case. Blue and yellow isosurfaces corresponds to the difference of spin-up and spin-down states

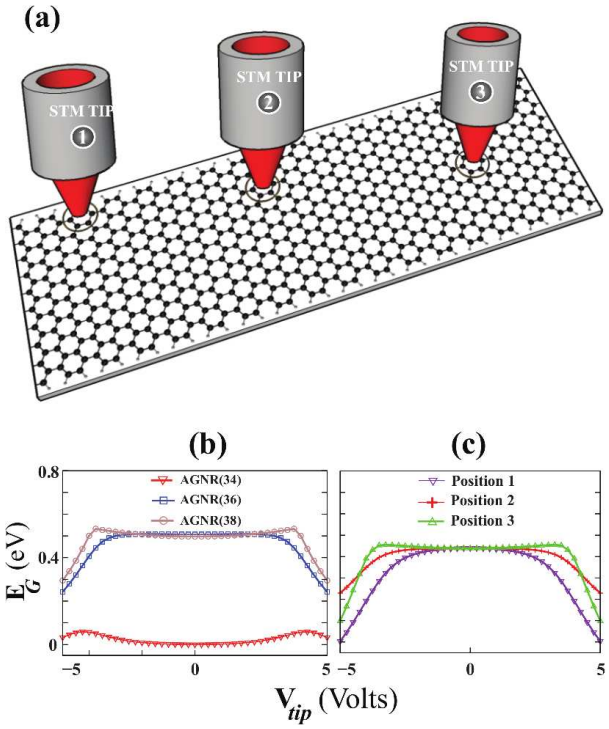

FIG. 5: (Color online) (a) Monitoring of band gaps E_G by applying a local bias voltage V_{tip} across the ribbon. (b) E_G versus V_{tip} applied at the center of AGNR(N;6) for N=34, 36 and 38. (b) E_G versus V_{tip} of AGNR(34) for different tip positions schematically described at the top. The tip (or electrodes) are situated at one of the position 1-3. The repeat period is l=20.

edges. In Fig. 4 (d)-(f) two defects associated with two separated vacancy and a defect associated with a relaxed divacancy exhibit similar behaviors.

An important issue to be addressed here is the breakdown of Lieb's theorem[21] for those zigzag ribbons. According to Lieb's theorem, the net magnetic moment per cell is determined with the difference in the number of atoms belonging to different sublattices, and it shall be either μ=1 μ_B or 2 μ_B for the cases in Fig. 4. None of the cases in Fig. 4 is in agreement with Lieb's theorem. Here one can consider two features, which may be responsible from this discrepancy. First is the strong Jahn-Teller distortion and relaxation of carbon atoms at the close proximity of the defect. As a result some dangling sp^2-bonds reconstructed to form new C-C covalent bonds. The lowering of the total energy, a driving force for such reconstruction, is as high as 0.5-0.6 eV/cell. Second is the interaction with the magnetic edge states, which becomes effective for narrow ZGNR's.

Finally, we note that introducing periodic vacancies or defects on a given ribbon appear to be difficult with the state of the art technologies. Here we propose a method as described in Fig. 5 to achieve the formation of periodic local defects like holes or vacancies. The sharp electrodes like STM tips are situated at desired locations, such as one of the cases 1-3 in Fig. 5 (a) on the graphene with a given repeat periodicity. A potential difference, V_{tip} common to all electrodes (tips) is applied between the tip and underlying insulator through the graphene. This way the electronic potential of graphene atoms just below the tip is locally lowered or raised depending on the polarity of V_{tip}. Here, the effect of locally and periodically applied potential difference has been modelled by ETB, where the on-site energies of carbon atoms below the tip have been changed accordingly. Although the present model is crude, it still allows us the realization of monitoring of the properties of nanoribbons. In Fig. 5 (b) the variation of E_G with V_{tip} is calculated for AGNR(N;20) with N=34, 36 and 38 by using period-

ically located tips at the center of the ribbon. Because of the electron-hole symmetry in the ribbons, the band gap variation depends on the magnitude of the bias voltage. In Fig. 5 (c) the variation of the band gap of AGNR(42;20) with V_{tip} and position of the tip is shown. In spite of the fact that the modifications of the band gaps are not the same as in Fig. 2, the available parameters, such as V_{tip}, l, tip-geometry and its position make the monitoring of the properties possible.

IV. CONCLUSIONS

In conclusion, we show that the energy band gaps and magnetic states of graphene nanoribbons can be modified by defects due to single or multiple vacancies. The optimized atomic structure of various vacancy defects have been found to be identical with the TEM images reported earlier[10]. Two different electronic states are distinguished: These are: (i) itinerant Bloch states perturbed by defects, (ii) defect induced states. While the former is dispersive, the latter give rise to flat bands. The reconstruction and spin-polarization of the orbitals at the close proximity of the defect give rise to net magnetic moments, which, in turn, changes the magnetic ground state of the defect-free ribbon.

Acknowledgments

Part of the computations have been carried out by using UYBHM at Istanbul Technical University through a grant (2-024-2007).

* Electronic address: ciraci@fen.bilkent.edu.tr

[1] K. S. Novoselov, A. K. Geim, S. V. Morozov, D. Jiang, M. I. Katsnelson, I. V. Grigorieva, S. V. Dubonos, A. A. Firsov, Nature **438**, 197 (2005).
[2] Y. Zhang, Y.-W. Tan, H. L. Stormer, P. Kim, Nature **438**, 201 (2005).
[3] C. Berger, Z. Song, X. Li, X. Wu, N. Brown, C. Naud, D. Mayou, T. Li, J. Hass, A. N. Marchenkov, E. H. Conrad, P. N. First, W. A. de Heer, Science **312**, 1191 (2006).
[4] M. I. Katsnelson, K. S. Novoselov, A. K. Geim, Nature Physics **2**, 620 (2006).
[5] A. K. Geim, K. S. Novoselov, Nature Materials, **6**, 183 (2007).
[6] Numerous studies have been carried out on the electronic structure of armchair and zigzag graphene ribbons. See for example: V. Barone, O. Hod and G.E. Scuseria, Nano Lett. **6**, 2748 (2006); Y.-W. Son, M.L. Cohen and S.G. Louie, Nature **444**, (2006); M. Y. Han, B. Ozyilmaz, Y. Zhang, and P. Kim, Phys. Rev. Lett. **98**, 206805 (2007).
[7] M. Fujita, K. Wakabayashi, K. Nakada, K. Kusakabe, J. Phys. Soc. Jpn. **65**, 1920, (1996).
[8] Y.-W. Son, M. L. Cohen, S. G. Louie, Phys. Rev. Lett. **97**, 216803 (2006).
[9] K. Nordlund, J. Keinonen, T. Mattila Phys. Rev. Lett. **77**, 699 (1996).
[10] A. Hashimoto, K. Suenaga, A. Gloter, K. Urita, S. Iijima, Nature **430**, 870 (2004).
[11] P. Esquinazi , D. Spemann, R. Höhne, A. Setzer, K.-H. Han, T. Butz, Phys. Rev. Lett. **91**, 227201 (2003).
[12] O. V. Yazyev and L. Helm, Phys. Rev. B **75**, 125408 (2007).
[13] X. Li, L. Zhang, S. Lee, H. Dai, Science **319**, 1229 (2008).
[14] X. Wang, Y. Ouyang, X. Li, H. Wang, J. Guo, H. Dai, Phys. Rev. Lett. **100**, 206803 (2008).
[15] P.E. Blochl, Phys. Rev. B **50**, 17953 (1994).
[16] J. P. Perdew, J. A. Chevary, S. H. Vosko, K. A. Jackson, M. R. Pederson, D. J. Singh, C. Fiolhais, Phys. Rev. B **46**, 6671 (1992).
[17] G. Kresse, J. Hafner, Phys. Rev. B **47**, 558 (1993).
[18] G. Kresse, J. Furthmüller, Phys. Rev. B **54**, 11169 (1996).
[19] As shown by the recent work based on self-energy corrections; L. Yang, C.H. Park, Y.-W. Son, M. L. Cohen, S. G. Louie, Phys. Rev. Lett. **99**, 186801 (2007); the band gap, E_G is underestimated by the DFT calculations. Since we consider structures which have already a band gap, its actual value does not affect our discussion in any essential manner.
[20] Using the definition of Schottky defect, we calculated the formation energy of relaxed vacancy of single carbon atom in AGNR(34) to be 7.79 eV. This value is smaller than the binding energy of a carbon atom in the graphene, which is calculated to be 9.23.
[21] E.H. Lieb, Phys. Rev. Lett. **62**, 1201 (1989).